# Lead-free piezoelectric material – $AgNbO_3$

A Project Report

submitted to the Department of Physics,

Indian Institute of Technology Hyderabad

as part of the requirements for the degree of

**MASTER OF SCIENCE**

By

**Digvijay Kharga**

Roll No. PH 12M1005

Under the supervision of

**Dr. Manish K. Niranjan and Dr. Saket Asthana**


DEPARTMENT OF PHYSICS

INDIAN INSTITUTE OF TECHNOLOGY HYDERABAD

INDIA

April, 2014

# Declaration

I hereby declare that the matter embodied in this report is the result of investigation carried out by me in the Department of Physics, Indian Institute of Technology Hyderabad under the supervision of Dr. Manish K. Niranjan and Dr. Saket Asthana.

In keeping with general practice of reporting scientific observations, due acknowledgement has been made wherever the work described is based on the findings of other investigators.

Digvijay Kharga

(Student's Signature)

Digvijay Kharga
(Student Name)
Roll No. PH12M1005

Manish K 24/04/14

Signature of the Supervisor

Dr. Manish K. Niranjan
Department of Physics,
Indian Institute of Technology Hyderabad,
Ordnance Factory Estate, Yeddumailaram- 502205,
Medak, Andhra Pradesh, INDIA

Saket Asthana
24/4/14

Signature of the Supervisor

Dr. Saket Asthana
Department of Physics,
Indian Institute of Technology Hyderabad,
Ordnance Factory Estate, Yeddumailaram- 502205,
Medak, Andhra Pradesh, INDIA

# Approval Sheet

This thesis entitled **"Lead-free piezoelectric material - $AgNbO_3$"** by Digvijay Kharga is approved for the degree of Master of Science from IIT Hyderabad.

Vandana Sharma ..... 25/04/2014

Name and affiliation V SHARMA IITM

Examiner

.....

Name and affiliation

Examiner

.....

Name and affiliation

Advisor

.....

Name and affiliation

Co-Advisor

.....

Name and affiliation

Chairman

# Acknowledgements

First and foremost, I offer my sincerest gratitude to my supervisors, Dr. Manish K. Niranjan and Dr. Saket Asthana, who have supported me throughout my project with their patience whilst allowing me the freedom to work in my own way. Their encouragement and immense knowledge were key motivations all throughout and has helped me a lot in cognitive learning and increasing interest in the field of research. I attribute the level of my Master's degree to their continuous assessment, encouragement and effort, which has instilled in me the sense of confidence, without which this project and thesis would not have been materialized.

I would also like to extend my appreciation to Mr. Kotagiri Gangaprasad and Mr. Durga Rao for assisting me and accompanying me in the due course of the project with their valuable assessments and experiences. They have been extremely helpful and have guided me a lot, and have been readily available for clearing doubts. I am also indebted to Mr. V. Sampath for sharing his understandings and helping me out in computational issues.

I would also like take this time to thank all my friends and group members for their support and encouragement. I also want to thank the Department of Physics, Physics Research Laboratory, Material Science Laboratory and IIT Hyderabad for extending their full support and providing the basic infrastructure and facilities for the project.

Finally, I would particularly like to thank my parents for supporting me all throughout and guiding me in every aspect of my life.

*Dedicated to my*

*Beloved parents*

# Abstract

In the present work, silver niobate ($AgNbO_3$), a potential lead-free piezoelectric material has been synthesized by conventional solid-state method. Dielectric and impedance studies of the compound in a wide frequency range and at different temperatures have been studied. Structural analysis confirms the single phase of the compound, with orthorhombic ($Pmc2_1$) crystal structure at room temperature. Microstructure and surface property of the sintered compound was investigated, and Raman measurements were also performed with the compound. Variation of dielectric constant with temperature at different frequencies, depicts the phase transitions that the compound undergoes. Frequency dependent studies of impedance $Z''$ (loss spectrum) shows the existence of strong dispersion in the relaxation time. In order to better understand the relaxation mechanism, Nyquist plots have been studied at temperature, $T \geq 360\ ^0C$ up to $400\ ^0C$. Relaxation time was found to decrease with increase in temperature and obey Arrhenius relationship. Variation in ac conductivity as a function of temperature was studied and activation energy was calculated.

# Table of Contents:-

- **List of figures**

## 1. Introduction :

Ferroelectric materials are subject to intense research for variety of applications due to their unique ferroelectric, piezoelectric, and pyroelectric properties. Out of the many potential applications microwave tunable dielectrics, sensors, non-volatile RAMs, dynamic capacitors, etc. are important ones. Mainly, lead based piezoelectric materials such as, lead zirconium titanate (PZT), lead zirconate, etc., are used for application purposes. However, due to environmental concern, there is growing interest in the development of high performance lead-free piezoelectrics. Recently, silver niobate ($AgNbO_3$) and its solid solutions with other compounds have been found very promising as a potential candidate for lead-free piezoelectrics with good electromechanical response. [4]

$AgNbO_3$ falls under the family **$ABO_3$** of perovskite type compounds. An ideal perovskite exhibits a cubic space group of *Pm3m*.

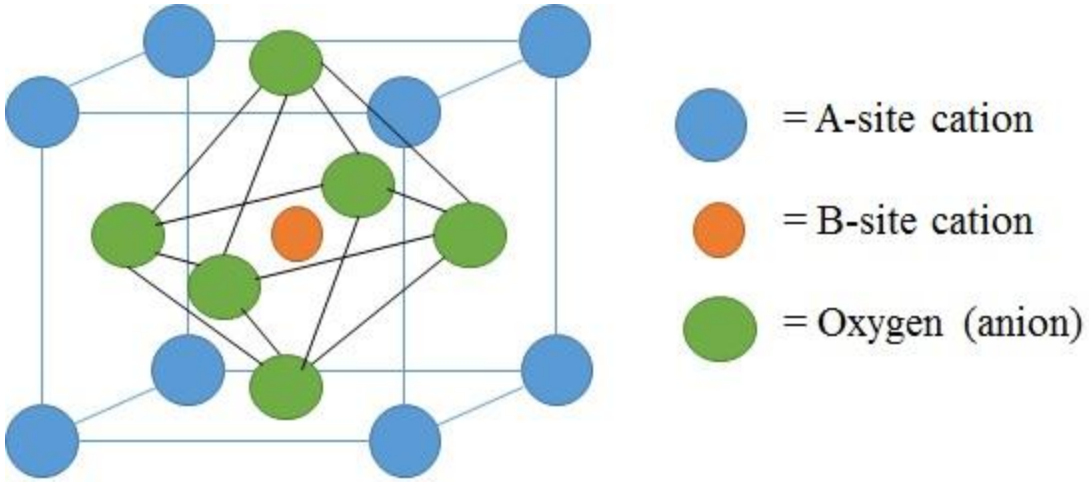


Fig.1.1: Ideal Perovskite Structure

This structure is centrosymmetric and does not allow the occurrence of ferroelectricity. But, there is always a ferroelectric instability in these type of compounds, guided mainly by the tolerance factor, $t = \frac{r_A + r_O}{\sqrt{2}(r_B + r_O)}$ defined by Goldschmidt, in 1926. Here, $r_A$ is radius of A-site cation, $r_B$ is radius of B-site of cation and $r_O$ is the radius of anion (oxygen). In ideal cubic paraelectric phase, it is equal to 1.

For $t < 1$ rhombohedral or orthorhombic distortions are found. In many cases, the structure adopts itself by tilting of the oxygen octahedra. For $t > 1$, the space available for the B-site cation in its octahedral "cage" is large enough so that it can rattle. This the simplest explanation of the origin of ferroelectric character in many perovskite compounds.

These type of compounds display a wide range of structural phase transitions, hence always has a tendency of ferroelectric instability. Silver niobate (AN) also undergoes a sequence of phase transitions, a paraelectric (cubic) - paraelectric (tetragonal), antiferroelectric (orthorhombic, *Pbcm*) - ferroelectric (orthorhombic, $Pmc2_1$) with decreasing temperature. So, the main aim of the project is to study the dielectric, impedance and ferroelectric properties of AN and henceforth, characterize the potential lead-free compound.

The phenomenology of the ferroelectric effect is predominantly based on the observation of an extremely high relative permittivity, which exhibits a maximum at a transition temperature usually designated as Curie temperature $T_C$. The most prominent theory in the description of ferroelectrics is **Ginzburg-Landau theory**.

The Ginzburg-Landau-Theory considers the interaction of many polar axes and introduces the polarization, *P* as an order parameter. Any crystal in thermodynamic equilibrium state can be completely specified in terms of a number of variables, for example temperature *T*, entropy *S*, electric field *E*, polarization *P*, stress $\sigma$, and strain *s*. The goal here is to write an *ansatz* for the free energy, $F_P = \frac{1}{2}aP^2 + \frac{1}{4}bP^4 + \frac{1}{6}cP^6 ..... - EP$

where, *E* is the electric field, and the unknown coefficients *a, b, c,* etc. are in general temperature-dependent and may have any sign. The equilibrium configuration is found out by finding the minima of *F*. The free energy of the system is expressed as an expansion of powers of this order parameter.

If all the coefficients, *a, b, c* are positive then, the free energy has a minimum at the origin (*E=0*). Hence, paraelectric in nature with no spontaneous polarization. [1]

Now, if the parameters are such that $a < 0; b, c > 0$, the free energy now will be of the form of a double-well. Hence, the ground state has a spontaneous polarization and is thus, ferroelectric. The demarcation between the two comes if *a* changes continuously with temperature,

and changes sign at a temperature $T_0$. Assuming *a(T)* varies linearly with temperature, say *a(T) = $a_0$ (T-$T_0$)*, $a_0$ is positive then, the dielectric susceptibility is given by, $\chi \propto \frac{1}{a} = \frac{1}{a_0(T - T_0)}$. Hence, a high dielectric constant value exists at the transition temperature, thus denoting a phase transition. This is an example of second order phase transition where the order parameter vanishes continuously at the transition temperature $T_C = T_0$.

For, *b < 0, c > 0*, it is clear that even if *T > $T_0$* i.e; *a* is positive, there can still be a subsidiary minimum existing at a non-zero P. As *a* is reduced (temperature lowered), this minimum will drop in energy to below that of unpolarized state and so will be the thermodynamically favoured configuration. The temperature at which this happens is the Curie temperature $T_C$, which however now exceeds $T_0$. This type of phase transition is called first-order or discontinuous transition, where the order parameter jumps discontinuously to zero at $T_C$.

**Coupling to Strain -** An important feature of ferroelectric materials is often their great sensitivity to elastic stress. Hence, we include the strain dependent terms in the expression for free energy, $F_S = \frac{1}{2} Ks^2 + (sP^2)d + .... - s\sigma$ . Here, *s* is the strain field (3x3 symmetric matrix with six independent components) and the first term accounts for elastic energy stored in a solid, the second term is a coupling between the elastic strain and polarization (lowest order of coupling allowed due to symmetry in this case). Returning to the total free energy, which now consists of $F_{tot}=F_P+F_S$ . The properties in equilibrium is determined by minimizing the free energy with respect to both *P* and *s*.

It is important to remember however that ferroelectricity is a property of the ensemble and not the individual parts, as a single unit cell is *per definitionem* incapable of ferroelectricity.

## 2. Experimental :

I. Preparation of pellets of $AgNbO_3$ :

$AgNbO_3$ (AN) ceramics were made using conventional solid-state reaction method. $Ag_2O$ and $Nb_2O_5$ were used as starting materials. Weighted powders in stoichiometric ratios were grinded using mortar and pestle for 2-3 hours using IPA (iso-propyl alcohol) and then calcinated at 980 $^0$C for 6 hours in oxygen atmosphere at 500 bars pressure. The phase formation of the sample was investigated using X-Ray Diffraction (XRD, X′Pert Pro, PANalytical) with Cu $K_\alpha$ radiation. Then, the calcined powder was ball-milled with PVA (poly-vinyl alcohol, binder) for 6 hours and pellets were prepared using Motorized Pellet Press (Kimaya Engineers) of diameter 8mm and 6mm. The pellets were then, sintered at 1150 $^0$C for 5 hours under the same conditions with a heating rate of 5 $^0$C/min. The density of the sintered pellets were higher than 95% of ideal density of $AgNbO_3$.

II. Microstructure of $AgNbO_3$ :

Micro-structure of $AgNbO_3$ was investigated with a Field Emission Scanning Electron Microscope (FE-SEM, Carl Zeiss SIGMA). A thin paste of silver was coated on the sample (sintered pellet) to make it conductive for measurements, and then properly mounted in the device. A small section of the sample was then selected and microstructure analysis were carefully made.

III. Raman measurements :

Raman measurements were done using Laser Micro Raman spectrometer (Bruker, Senterra). We used 532 nm laser light for this purpose with a laser spot size of 50 μm with a spectral resolution of 50 $cm^{-1}$. Only room temperature Raman studies were done with the samples of diameter 8 mm and thickness 1.5 mm.

IV. Impedance Spectroscopy :

For the electrical measurements, sample was coated with a thin silver paste. Temperature dependent dielectric constants and losses at various frequencies from 100Hz to 1MHz were measured with an Impedance Analyzer (Wayne Kerr, Model no. SSH-4C). Heating rate was maintained to be 5 $^0$C/min in the temperature range from room temperature to 400 $^0$C.

## 3. Results and Discussion :

### I. Structural Analysis and Microstructure :

Room temperature XRD pattern of AN ceramic is shown in **Fig. 3.1**. All the reflection peaks were indexed (with JCDS No. 520405) and confirmed that the structure of the sintered $AgNbO_3$ was found in good agreement of non-centrosymmetric orthorhombic structure ($Pmc2_1$), as also mentioned in previous structural studies. [2, 3]

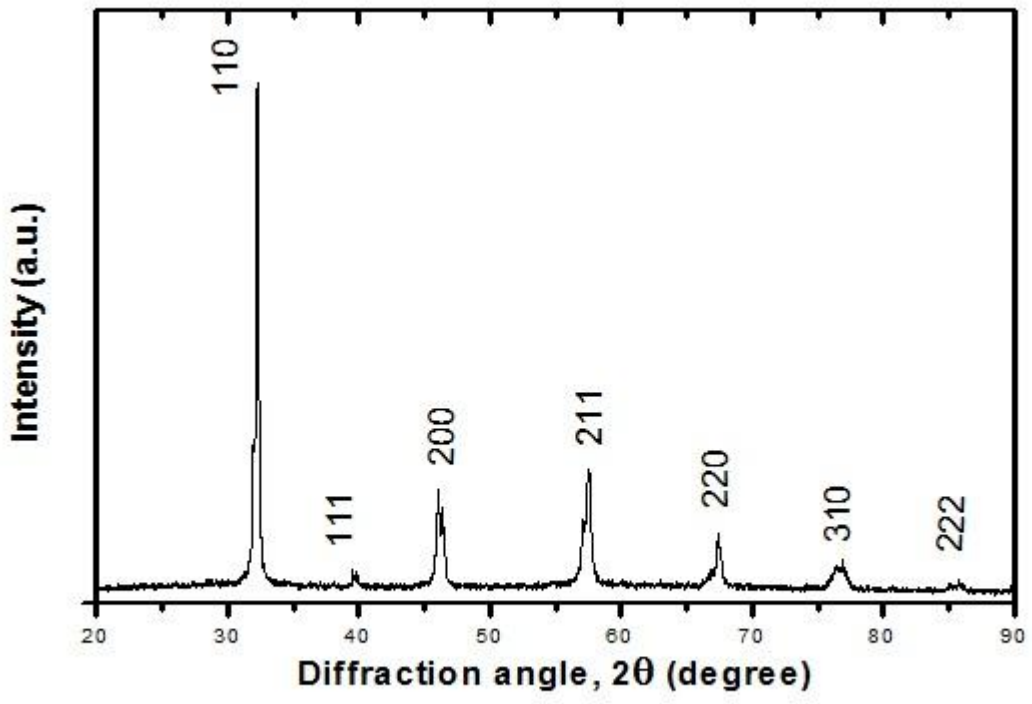


Fig.3.1: Room temperature XRD pattern of $AgNbO_3$

The lattice parameters of AN from XRD were calculated from the Bragg's diffraction formula, $2dsin\theta=n\lambda$ and are as follows:-

| a (Å) | b (Å) | c (Å) |
|---|---|---|
| 3.9422 | 3.9155 | 3.8771 |

Room temperature scanning electron micrograph at 10 kX magnification describing surface property and microstructure of AN is shown in **Fig. 3.2**. The grains were uniformly distributed throughout the sample showing its high compactness and polycrystallinity. The average grain size of the compound was ~2.16 μm. The presence of voids indicates that the sample pellet has certain amount of porosity.

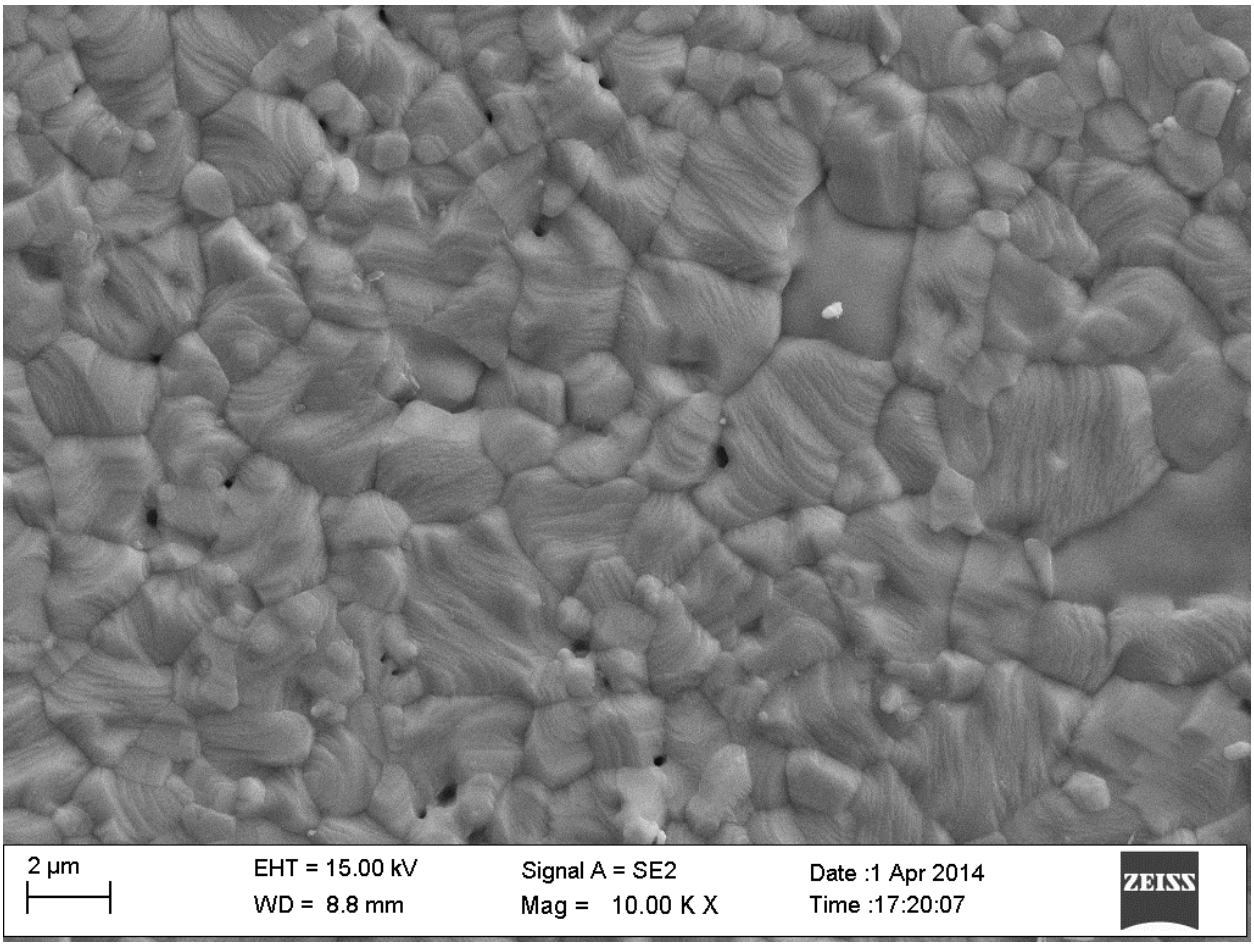


**Fig. 3.2**: SEM image of $AgNbO_3$ ceramic.

EDX (Energy Dispersive X-ray analysis) image is shown in **Fig. 3.3**. It confirms the stoichiometry of the sample $AgNbO_3$. Slightly less content of Silver is due to volatile nature of $Ag_2O$ (decomposition temperature of ~$220^0$C) and higher Oxygen content due to preparation of sample in $O_2$ atmosphere.

| Elements | Atomic % | |
|---|---|---|
| | Expected | Actual |
| Ag | 20 | 16.19 |
| Nb | 20 | 19.07 |
| O | 60 | 64.74 |

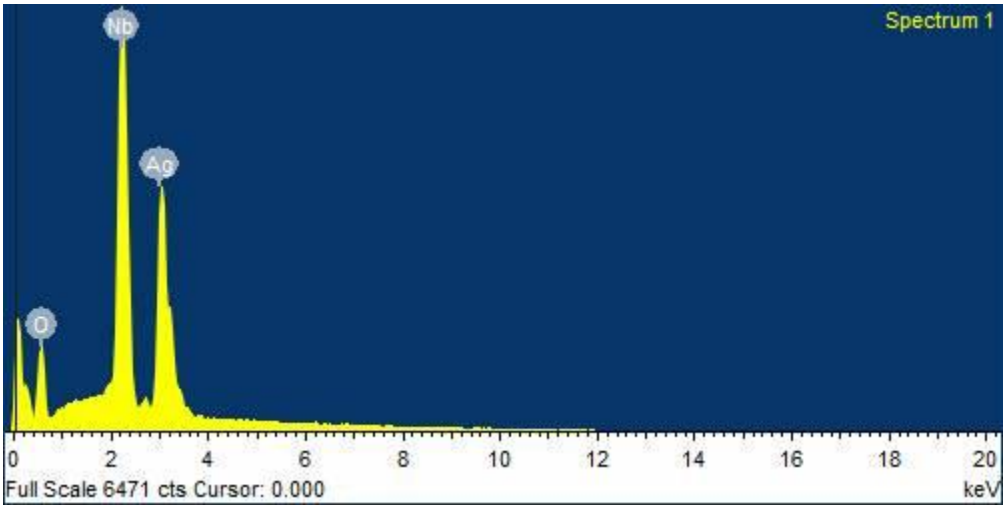


**Fig. 3.3**: EDX image of $AgNbO_3$

## II. Raman studies :

Raman scattering reveals about the rotational and vibrational modes in the system that are Raman active i.e. there is a change in polarizability due to the light-matter interaction. It is very commonly used because vibrational modes gives us specific information about chemical bonds and the symmetry of molecules.

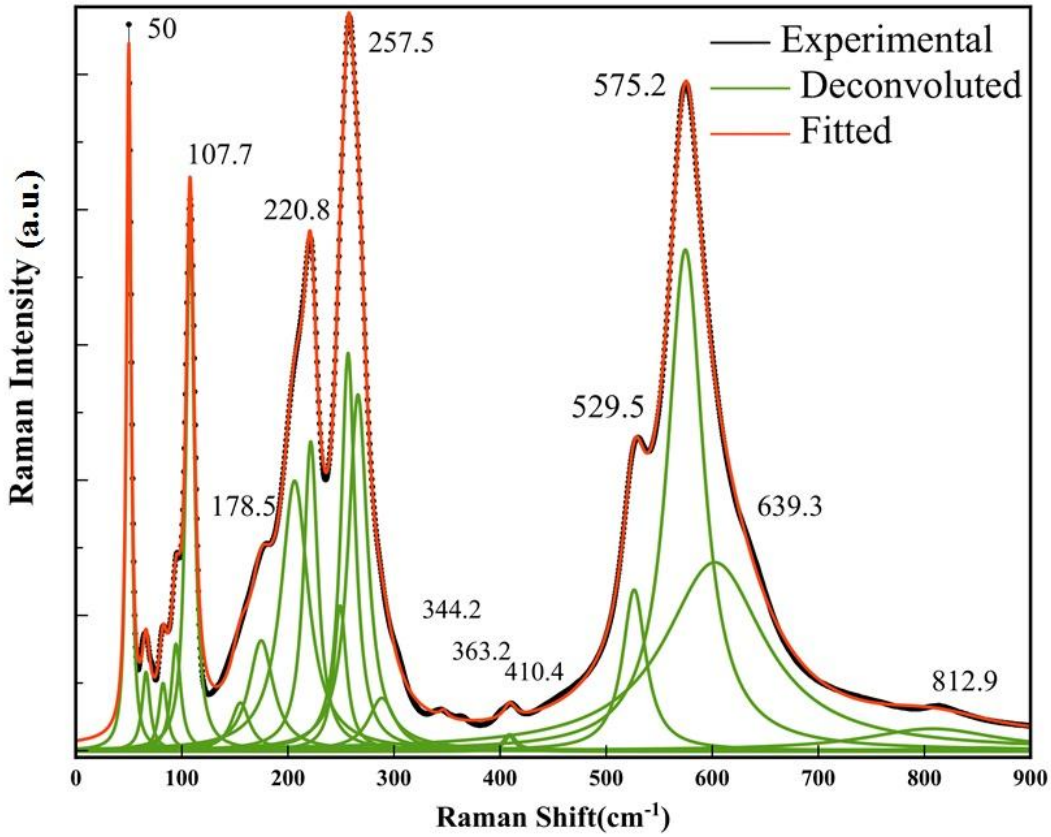


**Fig.3.4**: Raman scattering spectra of AN at room temperature.

Raman scattering spectra of AN at room temperature is shown in **Fig. 3.4**. The spectra is deconvoluted with the help of multiple Lorentzian plots and then, the final deconvolved spectra is shown above with different modes. The spectra exhibit a complicated structure with many peaks which can be divided into three main ranges :-

(a) a low-frequency part below 120 $cm^{-1}$

(b) an intermediate one between 150 and 300 $cm^{-1}$

(c) a high-frequency range above 500 $cm^{-1}$.

Room temperature Raman spectra does not reveal much, but the central peak maxima is due to the Nb ion motions. [15] The role of the silver ion has to be considered taking into account the complex sequence of phase transitions. Theoretical calculations are needed for better understanding about the room temperature spectra.

## III. Dielectric studies :

From the temperature dependent dielectric constant ($\varepsilon'$), phase transitions were studied as shown in the **Fig. 3.5**. The peak in the value of $\varepsilon'$ corresponds to a phase transition. Here, $\varepsilon'$ is calculated from the formula, $C = \varepsilon_0 \varepsilon' \left( \frac{A}{d} \right)$ => $\varepsilon' = \left( \frac{C}{C_0} \right)$ where, $C$ is the capacitance of the pellet (sample), $\varepsilon_0$ is permittivity of free space, $A$ is the area of the sample and $d$ is the thickness, $C_0$ is capacitance due to free space.

A sequence of phase transitions were observed for silver niobate, M-1, M-2 and M-3 denoting orthorhombic M-phases, O-1 and O-2 denoting orthorhombic O-phases, and T is tetragonal phase.

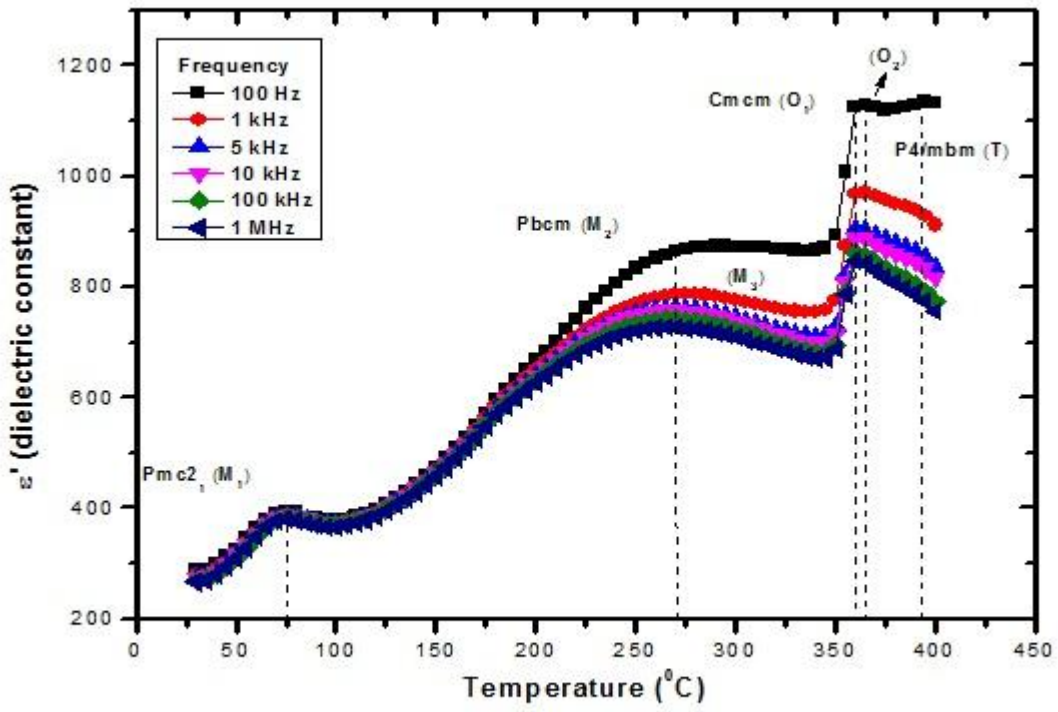


Fig. 3.5: Dielectric dispersion of $AgNbO_3$

For 100Hz, at 75 $^0$C, M-1 to M-2 transition was observed. A diffused phase transition from M-2 to M-3 was observed at ~270 $^0$C. Further, two orthorhombic phase transitions, first from M-3 to O-1 at 360 $^0$C and second from O-1 to O-2 at 365 $^0$C, were observed. Then, a phase transition from

O-2 to T was observed at 395 $^0$C. All the phases reported before have been observed in the plots. [2-5] It was observed that the $\varepsilon'$ increases with increase in temperature showing anomaly at the transition temperature. The peak height at the transition temperature was observed to decrease with increasing frequency, and the dielectric constant peak shifted to lower temperature with increasing frequency, which indicated the relaxation behavior of the material.

Dielectric loss is the dissipation of energy through the movement of charges in an alternating electromagnetic field as polarization switches direction and is given by, $\varepsilon'' = \varepsilon'(\tan\delta)$. **Fig. 3.6** shows the variation in the loss factor (tanδ) with temperature. The loss factor increases with temperature (tends to be higher for higher dielectric constant values), and the effect is more prominent in the lower frequency domain because of space charge polarization.

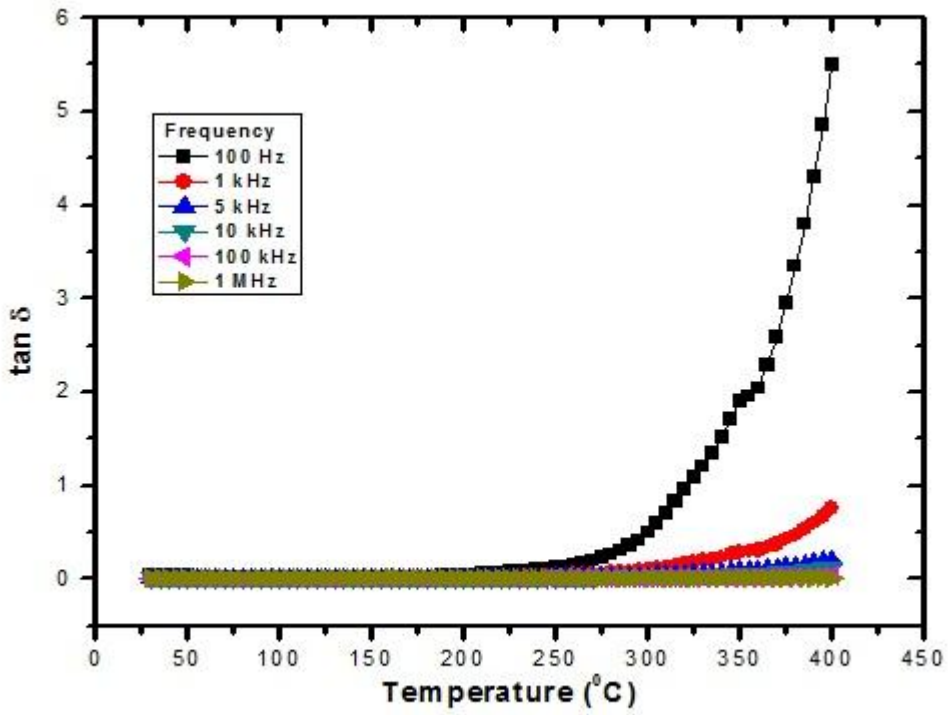


Fig. 3.6: Temperature dependence of loss factor (tanδ)

**Fig. 3.7** shows frequency dependence of dielectric constant ($\varepsilon'$), at different temperatures. It was observed that $\varepsilon'$ gradually decreases as the frequency increases in a given temperature range. The decrease in $\varepsilon'$ is due to the space charges, because within this frequency range (100Hz – 1MHz) the major contribution is due to space charge polarization which leads to high dielectric constant and significant frequency dispersion. On increasing temperature, $\varepsilon'$ increases apparently which becomes even more significant at low frequency. This indicates thermally activated nature of the dielectric relaxation of the system.

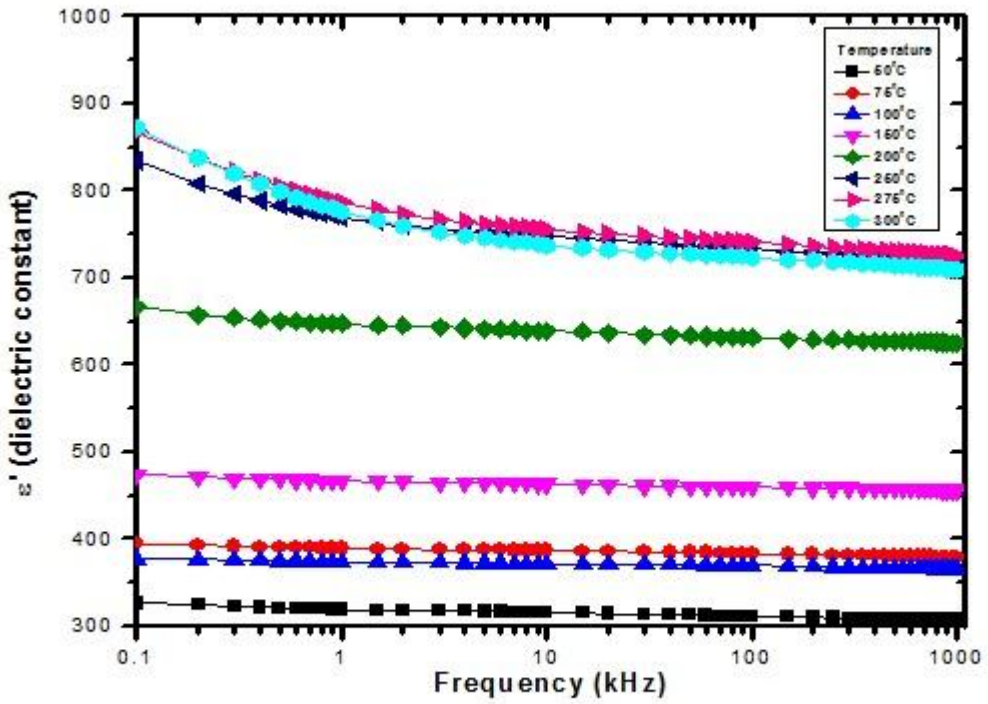


Fig. 3.7: Frequency dependence of ε' at different temperatures

**Fig. 3.8** shows the variation of the loss factor (tanδ) with frequency at different temperatures. It was observed that the loss factor decreases with the increase in frequency is due dipolar lagging taking place in the material which is common in most ferroelectrics. All the values of tanδ merge at higher frequency domain, as here the space charge polarization mechanism is unable to keep the switching electric field, and hence its contribution towards dielectric constant above this frequency is negligible. [9]

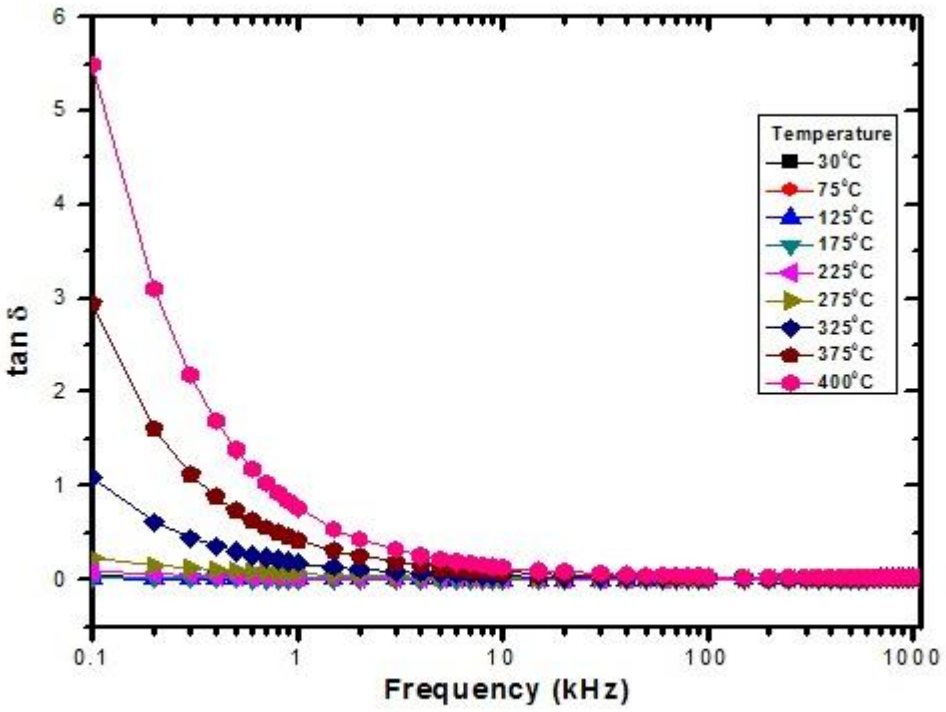


Fig. 3.8: Frequency dependence of tanδ at different temperatures

## IV. Impedance studies :

Impedance spectroscopy is a powerful and versatile technique to analyze the electrical property of dielectrics as it distinguishes between intrinsic (bulk) and extrinsic (grain boundary, surface layer and electrode) contributions. Various relaxation processes coexists in real crystals or ceramics, and hence the departure of their response, from the ideal Debye model resulting from the interaction between dipoles, cannot be discarded.

**Fig. 3.9** shows frequency dependence of $Z'$ at different temperatures. At low frequency, real part of impedance $Z'$ increases with the increase of temperature and then, these values merge at high frequency region due to the increase in the ac conductivity i.e. existence of negative temperature coefficient of resistance (NTCR) in the compound. Here, the effective impedance decreases with increase in temperature.

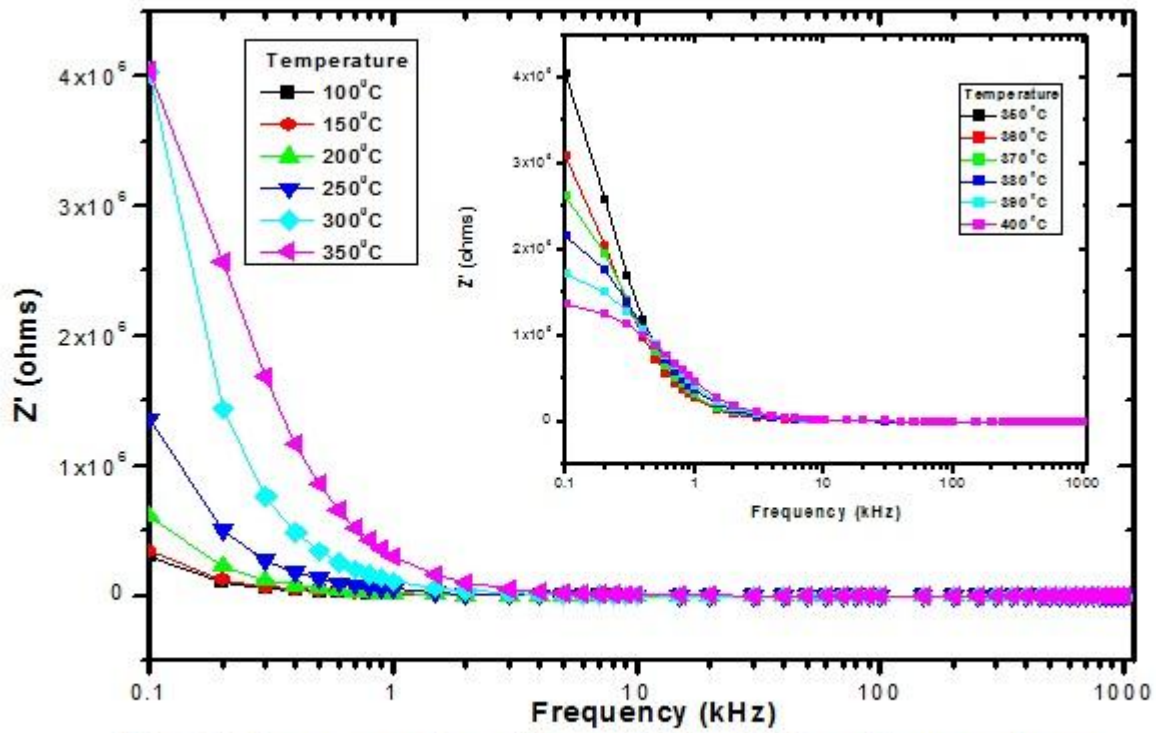


Fig. 3.9: Frequency dependence of Z ' at different temperatures

In **Fig. 3.10** frequency dependence of $Z''$ at different temperatures is shown, and it is observed that position of $Z''$ peak shifts to higher frequency side on increasing temperature, this effect is even more pronounced at higher temperatures $\geq 350^0$C (at ~ M-3 to O-1 transition) thus, denoting distribution of relaxation time. Here, decrease in the magnitude of $Z''_{max}$ is due to enhanced conductivity at higher temperatures (above 350 $^0$C) and peak shifting to the right is due to decrease in the relaxation time ($\tau$). The frequency $\omega_{max}$ (corresponding to $Z''_{max}$) gives the relaxation time $\tau$, from the condition $\omega_{max}\tau_m = 1$. [7]

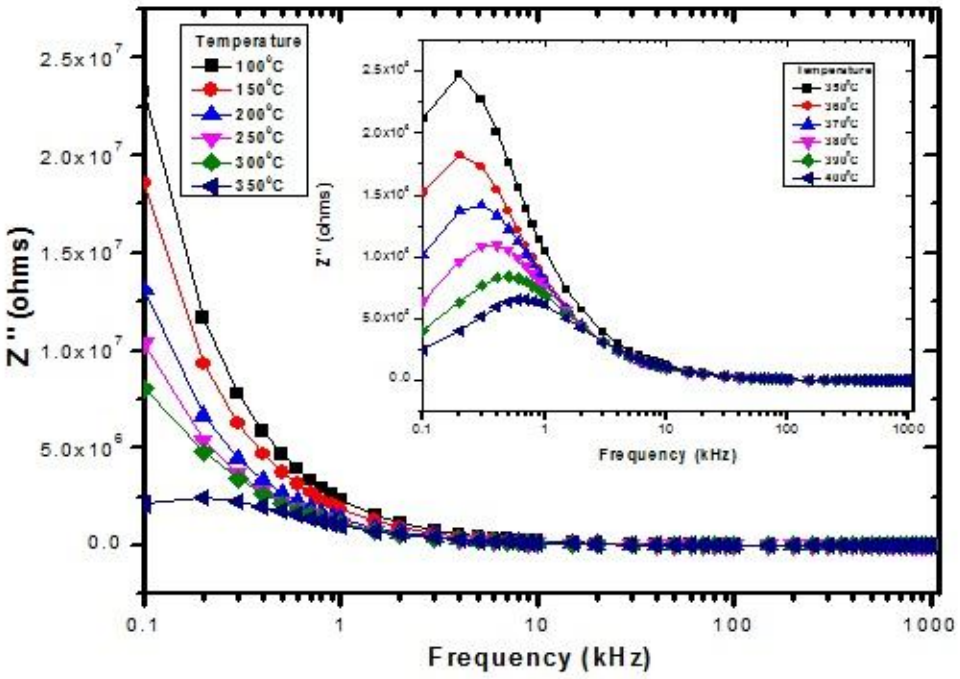


Fig. 3.10: Frequency dependence of Z " at different temperatures

Scaling behavior of $Z''$ at different temperatures is depicted by the **Fig. 3.11** and from the figure it is evident that as the temperature increases the peak frequency of $Z''/Z''_{max}$ does not shift, revealing that higher temperature does not trigger another relaxation process within this range of temperature and frequency. Furthermore, the perfect overlap of all the curves for all the temperature into a single master curve indicates that the relaxation mechanism is the same at different temperatures. [7]

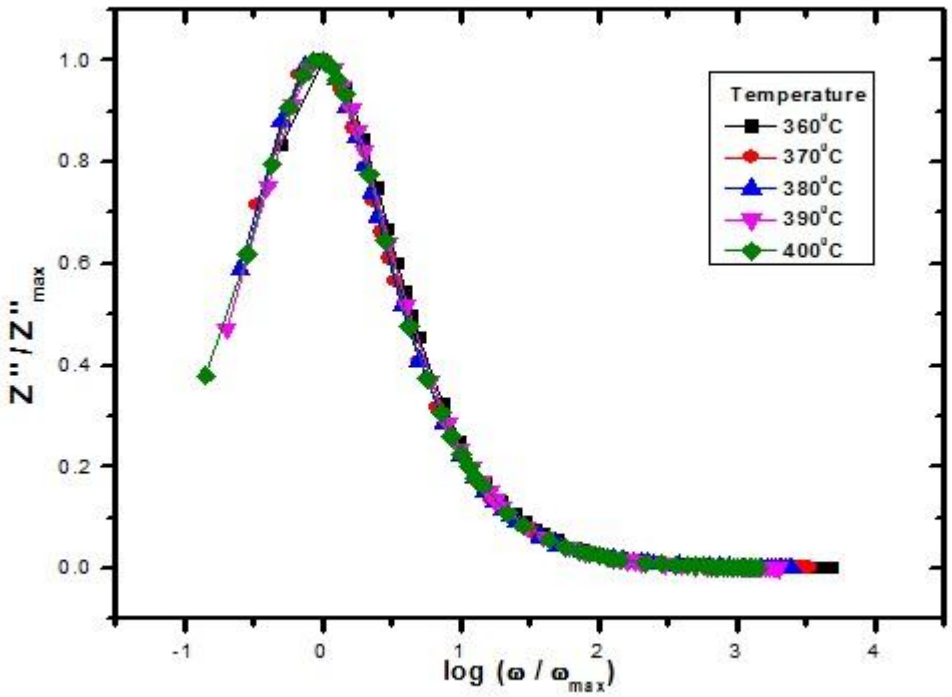


Fig.3.11: Normalized imaginary part of impedance ($Z''/Z''_{max}$) as a function of $\log(\omega/\omega_{max})$

## V. Dielectric Relaxation :

Relaxation means a system's monotonous approach to the equilibrium state after some excitation. In the case of dielectric relaxation, it is the response of polarization to an external (usually small) electric field. Relaxor ferroelectrics, or relaxors, are a class of disordered crystals possessing peculiar structure and properties. It is typically related to the dynamics of "elementary" electric dipole of molecules, ions, or electrons hopping among the allowed potential wells. In case of orientational polarization, the directions vary rapidly (manifestation of thermal motion), so that time-average values ‹ $\mathbf{p_i}$› equal zero and electric polarization, which is defined as the dipole moment density, $\mathbf{P} = \sum$‹ $\mathbf{p_i}$›/ $\mathbf{V}$, also equals zero. An applied electric field (E) tends to align elementary dipole moments in a particular direction, but complete alignment can only be obtained practically in a very large E exceeding the breakdown field of the material. Under small fields typically used to study dielectric relaxation, every elementary dipole continues its reorientational motion, but spends more time being in the directions parallel (or almost parallel) to E, so that ‹ $\mathbf{p_i}$› becomes nonzero and a macroscopic P appears. The time necessary for P to develop (macroscopic relaxation time) is determined by the rate of thermally activated flipping of elementary dipoles, i.e. by the depth of the associated potential wells. [11]

The polycrystalline materials usually have grain and grain boundary properties. In order to further investigate the relaxation mechanisms, complex plane plots (Cole-Cole and Nyquist diagrams) can be plotted wherein these contributions can be conventionally displayed. At high temperatures, two successive semicircles may occur due to these properties. [7]

Complex impedance:

$$Z^*(\omega) = Z' - jZ''$$

where,

$$Z' = |Z|\cos\theta \quad \text{and} \quad Z'' = |Z|\sin\theta$$

Complex permittivity:

$$\varepsilon^*(\omega) = \varepsilon' - j\varepsilon'' \qquad \text{and} \qquad \tan\delta = \frac{\varepsilon''}{\varepsilon'} = -\frac{Z'}{Z''}$$

**Fig. 3.12** shows a set of Nyquist plots ($Z'$ vs $Z''$) over a wide range of frequency (100Hz - 1 MHz) at different temperatures. The effect of temperature on impedance and related parameters of materials becomes clearly visible with rise in temperature. On increasing temperature, the slope of the lines decreases, and hence they bend towards $Z'$-axis by which semicircle could be formed. At higher temperatures (≥ 350 $^0$C), it was possible to trace the semicircle. The intercept of the semicircle on the real axis is the bulk resistance ($R_b$) of the sample.

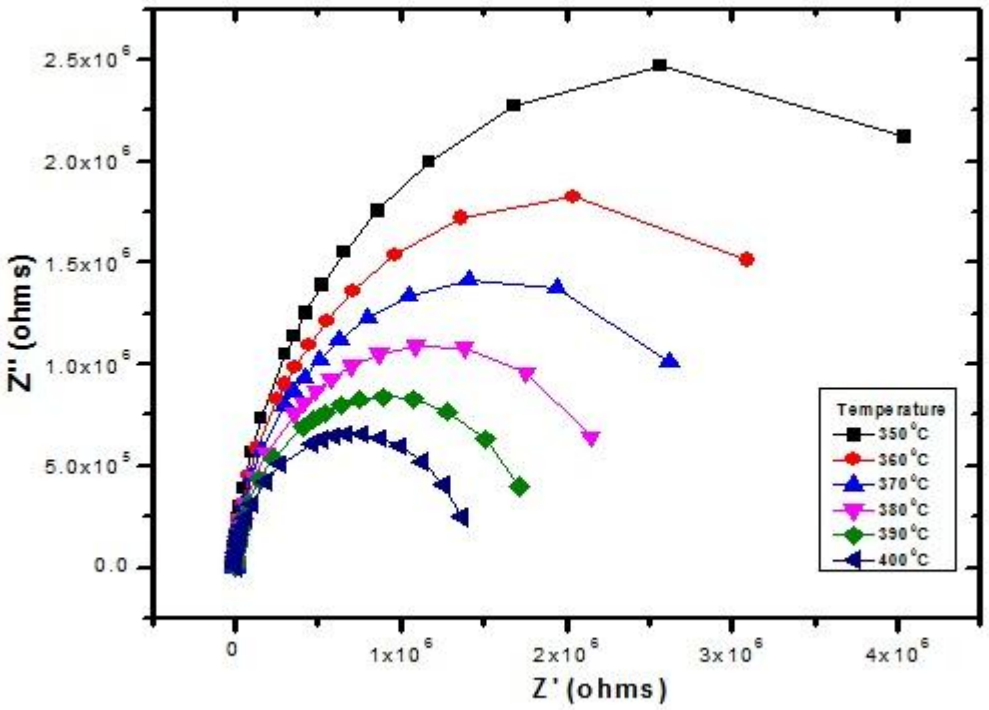


Fig.3.12: Nyquist plots (Z' vs Z") at different temperatures

The presence only one semi-circle in the Nyquist plot confirms that the polarization mechanism in AN corresponds mainly due to the bulk effect arising in semi-conductive grains. [14]

The table below shows the variation of grain resistance, grain capacitance and relaxation time with temperature from the fitted Nyquist plots with an equivalent RC circuit. It also confirmed that in this compound, the relaxation time decreases with increase in temperature.

| Temp. ($^0$C) | Grain resistance ($R_g$) in MΩ | Grain Capacitance ($C_g$) in pF | Relaxation time ($\tau = R_gC_g$) in μ-sec |
|---|---|---|---|
| 350 | 5.397 | 40.64 | 219.34 |
| 360 | 4.008 | 52.07 | 208.70 |
| 370 | 3.121 | 51.79 | 161.66 |
| 380 | 2.404 | 50.62 | 121.71 |
| 390 | 1.844 | 49.68 | 91.60 |
| 400 | 1.432 | 48.07 | 68.82 |

The relaxation behavior is close to Debye relaxation (with $\alpha \rightarrow 0$) as the Nyquist plots were nearly a pure single semicircle.

## VI. Conductivity studies :

Ac conductivity measurements have been widely used to investigate the nature of ionic motion in materials since they are responsible for this type of conduction. **Fig. 3.13** shows the frequency dependence of ac conductivity ($\sigma_{ac}$) of AN ceramic at different temperatures. The ac electrical conductivity was calculated by using the relation, $\sigma_{ac} = \frac{d}{AZ'}$ where, *d* is the thickness and *A* is the surface area of the pellet. At low temperatures, low frequency plateau and high frequency dispersion of conductivity was observed. At higher temperatures, broader plateau in low frequency region was observed and dispersive behavior of conductivity irrespective of temperature at higher frequency region. The plateau region corresponds to frequency independent dc conductivity ($\sigma_{dc}$) and dispersive region corresponds to frequency dependent part, which can be clearly observed in **Fig. 3.13**(inset). [7, 14] At low frequency (up to 300 Hz), conductivity increases with temperature showing thermally activated nature of the conduction process.

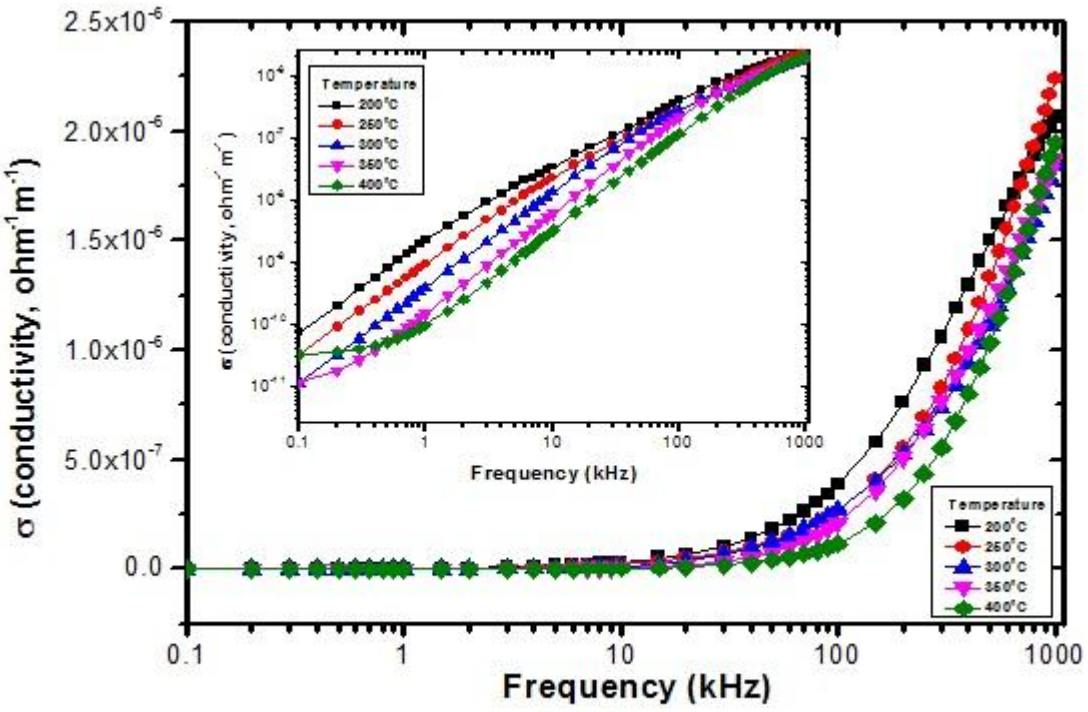


Fig.3.13: Variation of ac conductivity of AN at different temperatures

## VII. Arrhenius study :

Arrhenius equation is a simple but remarkably accurate formula for temperature dependence of reaction rates. It give the dependence of rate constant $K$ as, $\mathbf{K = A * exp (-E_a/k_BT)}$ where, $A$ is the pre-exponential factor, $k_B$ is the Boltzmann constant, $T$ is absolute temperature (Kelvin), and $E_a$ is the activation energy. Arrhenius argued that for reactants to transform into products, they must first acquire a minimum amount of energy, called the activation energy $E_a$. At an absolute temperature $T$, the fraction of molecules that have a kinetic energy greater than $E_a$ can be calculated from statistical mechanics. The concept of *activation energy* explains the exponential nature of the relationship, and in one way or another, it is present in all kinetic theories.

The relaxation time $\tau_m$ is calculated from fitted Nyquist plot. **Fig. 3.14** shows the variation of relaxation time as a function of temperature. The relaxation time follows the Arrhenius law given by, $\mathbf{\tau_m = \tau_0 * exp (E_a/k_BT)}$.

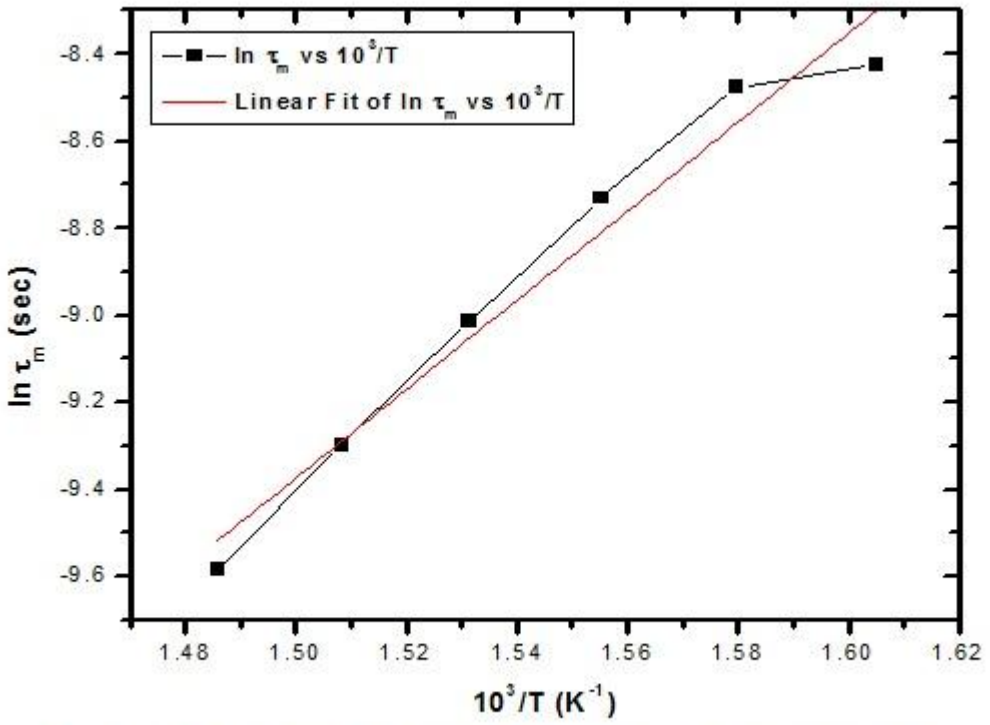


Fig.3.14: Variation of relaxation time ($\tau_m$) with temperature

**Fig. 3.15** shows the variation of dc conductivity of AN (calculated from the values of σ at various peak frequencies) as a function of temperature. The peak dc conductivity also follows the Arrhenius law given by, $\sigma_{dc} = \sigma_0 * \exp(-E_a/k_BT)$ where $\sigma_0$ is the pre-exponential factor, $k_B$ is the Boltzmann constant and $E_a$ is the activation energy.

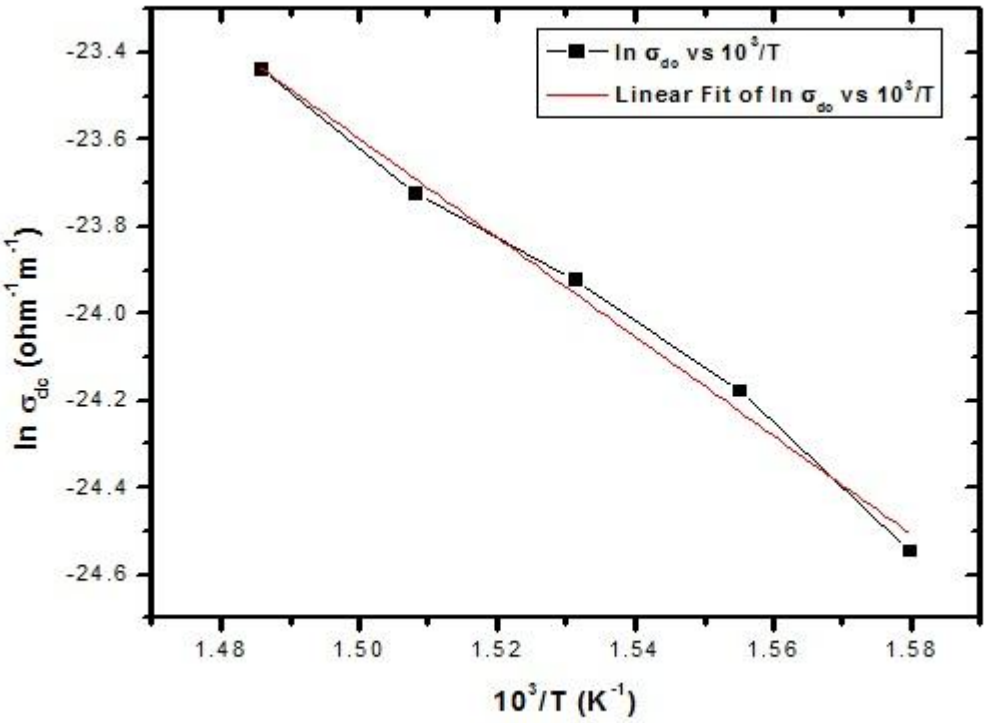


**Fig.3.15: Variation of dc conductivity ($\sigma_{dc}$) with temperature**

The activation energy ($E_a$) calculated from the linear best fit of the plots in **Fig. 3.14** and **Fig. 3.15** was found out to be 0.8804 eV and 0.9813 eV respectively. The activation energy calculated from the two plots are approximately equal. [7]

## 4. Conclusions :

Polycrystalline $AgNbO_3$ was prepared by solid state synthesis route and it crystallizes into *Pmc2₁* space group at room temperature. SEM indicates that the compound has almost uniform grain size of ~2.16 μm. Room temperature Raman scattering spectra does not reveal much information. Phase transitions of AN were confirmed with the help of dielectric studies and further, impedance studies of the samples via Nyquist plots reveal that the relaxation mechanism is mainly due to bulk effect arising in semi-conductive grains. The ac conductivity studies reveals the conduction process is thermally activated. Further, the activation energy ($E_a$) was calculated from the Arrhenius plot of relaxation time and dc conductivity, and they both agree very well.

The ferroelectric and piezoelectric behavior of pure $AgNbO_3$ needs to be investigated using *D-E* and *S-E* hysteresis loops, as it could not be completed due to breakdown of the samples at 3kV/cm potential difference only. In order to better understand the room temperature Raman spectra, theoretical calculations are needed to be done, so that a better correlation can be made with different modes of vibration.

## 5. References :


[1] K. M. Rabe, C. H. Ahn, and J. M. Triscone, Physics of Ferroelectrics.

[2] P. Sciau, A. Kania, B. Dkhil, E. Suard, and A. Ratuszna, J. Phys.: Condens. Matter **16**, 2795 (2004).

[3] I. Levin, V. Krayzman, J. C. Woicik, J. Karapetrova, T. Proffen, M. G. Tucker, and I. M. Reaney, Phys. Rev. B **79**, 104113 (2009).

[4] D. Fu, and M. Itoh, Ferroelectricity in Silver Perovskite Oxides.

[5] K. H. Ryu, J. A. Cho, T. K. Song, M. H. Kim, S. S. Kim, H. S. Lee, S. J. Jeong, J. S. Song, and K. S. Choi, Ferroelectrics **338**, 57 (2006).

[6] K. C. Kao, Dielectric Phenomenon in Solids.

[7] S. K. Barik, R.N.P. Choudhary, and A.K. Singh, Adv. Mat. Lett. **2**(6), 419 (2011).

[8] R. Sagar, and R.L. Raibagkar, J. Alloys Compd. **549,** 206 (2013).

[9] P. Kumar, B. P. Singh, T. P. Sinha, and N. K. Singh, Physica B **406**, 139 (2011).

[10] D. Fu, M. Itoh, and S. Koshihara, J. Appl. Phys. **106**, 104104 (2009).

[11] A. A. Bokov, and Z. G. Ye, J. Adv. Dielectr. **2**(2), 1241010 (2012).

[12] D. Schutz, and K. Reichmann, J. Ceram. Soc. Jpn. **122**(4), 231 (2014).

[13] M. K. Niranjan, and S. Asthana, Solid State Commun. **152**, 1707 (2012).

[14] L. Agarwal, B. P. Singh, and T. P. Sinha, Mat. Res. Bull. **44**, 1858 (2009).

[15] A. Kania, K. Roleder, G. E. Kugeli, and M. D. Fontanat, J. Phys. C: Solid State Phys. **19**, 9 (1986).